Stability analysis of conducting jets under ac radial electric fields for arbitrary viscosity

Heliodoro González[a]
Departamento de Física Aplicada III, E.S.I., Universidad de Sevilla, Camino de los Descubrimientos, s/n 41092, Sevilla, Spain
and Departamento de Electrónica y Electromagnetismo, Facultad de Física, Universidad de Sevilla, Avenida Reina Mercedes, s/n 41012, Sevilla, Spain

F. Javier García
Departmento de Física Aplicada I, E.U.I.T.A., Universidad de Sevilla, Carretera de Utrera, km. 1, 41013, Sevilla, Spain
and Departamento de Electrónica y Electromagnetismo, Facultad de Física, Universidad de Sevilla, Avenida Reina Mercedes, s/n 41012, Sevilla, Spain

Antonio Castellanos
Departamento de Electrónica y Electromagnetismo, Facultad de Física, Universidad de Sevilla, Avenida Reina Mercedes, s/n 41012, Sevilla, Spain

A temporal linear modal stability analysis is presented for conducting viscous liquid jets flowing with nonzero velocity relative to an ambient gas and subjected to an ac radial electric field. Parametric resonance between natural dc frequencies and the frequency (or multiple) of the imposed ac field eventually leads to destabilization of the jet for perturbations with wave numbers in the stable domain. In this way, it is possible to obtain drops of smaller size. The main result is the extension of the stability analysis to liquids of arbitrary viscosity using a dynamical approach, instead of previous variational models valid for slightly viscous liquids. The effect of the outer gas in relative motion is taken into account in the framework of currently available semiempirical theories. A brief discussion of the dispersion relation for dc fields is included as the natural starting point for the discussion of the ac case. Use of the 1-D averaged model for axisymmetric perturbations, an alternative to the 3-D approach, allows a complete determination, in this particular case, of the distribution and nature of roots of the dispersion relation in the complex plane. The theoretical study presented here is ready to be compared to future experiments in the Rayleigh and first wind-induced regime, as no relevant instability mechanisms have been excluded; namely, capillary instability, viscous damping, quasi-electrostatic pressure effects, Kelvin–Helmholtz instability corrected to account for the gas viscosity, and finally, parametric resonance. © *2003 American Institute of Physics.* [DOI: 10.1063/1.1529659]

I. INTRODUCTION

The application of electric fields is at present widely used in ink jet printing technologies as a method for charging and deflecting the ink drops resulting from jet disintegration.[1] Electric forces may also be applied to select perturbations with a specific wavelength, a mechanism alternative to piezoelectric stimulation.[2] For this purpose, sharp electrodes close to the jet surface establish a locally strong alternating field; the time-varying quasi-eletrostatic pressure jump induces a perturbation whose frequency, along with the jet velocity, determines the selected wavelength. Also, in the same configuration, an electric pulse has revealed to be useful for obtaining isolated drops inside a continuum jet.[3–5] These applications, among others, have motivated the interest of the EHD researchers' community in electric forces acting on conducting jets. Conducting jets in the presence of radial electric fields have been studied since the work of Melcher,[6] where liquids were restricted to be inviscid and the imposed electric potential was supposed constant in time. The effect of viscosity was later included by Saville.[7] This linear stability analysis has been more recently revisited by García,[8] who conducted a thorough study of the resulting dispersion equation in all the relevant parameters; in addition, in his work can be found a comparison with one-dimensional models that are validated as a computationally economic approach to the nonlinear jet dynamics. Besides, alternating fields have been considered by González *et al.*[9] in the hope that parametric resonances give new tools for the jet breakup control. The main objective was to reduce the size of the final drops. In this latter work, a variational approach (using the Lagrangian method introduced by Lord Rayleigh[10]) was employed to formulate the linear stability problem for the restricted conditions of slightly viscous liquid and a negligible outer medium.

However, the effect of the surrounding gas in relative motion on a jet is not negligible in many experimental situ-

[a]Electronic mail: helio@us.es

ations. The first attempt to account for it was done by Weber[11] by introducing the Kelvin–Helmholtz instability mechanism with the assumption of a zero gas viscosity. Sterling and Sleicher[12] corrected the resulting dispersion relation and included the effect of a small viscosity of the gas in a semiempirical way. Based on the results found by Benjamin[13] for a planar geometry, these authors modified the instability mechanism by considering a reduction in the normal stress exerted by the gas on the free surface. The reduction coefficient does not come from a rigorous derivation, which still remains as an unaddressed theoretical issue. A recent work[14] provides the linear stability analysis of liquid and gas basic flows, characterized by nonuniform velocity profiles numerically calculated, for the related problem of a jet co-flowing in a gas stream, but there are neither results for small aerodynamic Weber numbers nor an explicit comparison with the results of Sterling and Sleicher, whose model we adopt in this paper.

The problem we now formulate may be considered as the natural end of the sequence that we have just described: ac fields, arbitrary viscosity and surrounding gas dynamics are all together taken into account. But, for this general problem, the variational method is not suitable because the velocity field of a viscous liquid is no longer potential, a necessary condition to apply it. Instead, the starting point will be the linearized Navier–Stokes equations, as in Refs. 7 and 8. In fact, a generalization of the dispersion equations therein found for dc fields for including the effects of the outer gas previously derived and used as a reference to better understand the ac case.

It is well-known that systems driven by time-varying, periodic forces exhibit in general a resonant behavior for selected values of the force strength parameter. For this reason we use expressions such as "parametric instability" or "parametric resonance." Faraday resonance in a liquid layer subjected to periodic vertical motion as a whole enters in this category, as well as our present problem. In fact, the reader can find a parallel between the resolution proposed here and recent publications on Faraday resonance in viscous liquids.[15–17] The basic mathematical tool in all these works is a direct application of Floquet's theory to the governing partial differential equations, which leads to a splitting of all unknowns into an exponential time dependence multiplied by a periodic function of time, with subsequent Fourier decomposition of the latter. Here, solutions are obtained in the form of rapidly converging continued fractions, whose terms are directly related to the dispersion equation for the dc problem. In those references, the authors pay attention only to the loci in the parameter space leading to periodic (nongrowing) solutions, i.e., the marginal stability analysis. However, in our case, the growth rates of the jet perturbations are essential information, which we obtain by exploiting the same technique.

Aside from the three-dimensional (3-D) analysis, which gives results valid for any wavelength of the jet perturbations, one-dimensional (1-D) models rigorously developed by García and Castellanos[18] are employed to reobtain these results. The main assumption of 1-D models is that the wavelength λ must be much greater than the unperturbed jet radius R; this restriction is not as severe as one could think and the 1-D approach remains useful for a range of wavelengths typical in experiments with periodically stimulated jets ($2\pi R/\lambda \gtrsim 1$). In any case, the structure of parametric resonances as a function of the wavelength of perturbations is well described; and the simplicity of the dispersion relations that we have to handle makes 1-D models an excellent tool to understand the role of each parameter.

The paper is organized as follows. Section II presents the problem formulation along with the basic solution. In Sec. III, the stability analysis about this basic state is carried out in two steps: first for the dc case (starting with a zero-field solution and then adding the electric field influence) and later for the ac case. In this same section, we propose an alternative 1-D treatment to obtain the dispersion relation for the axisymmetric case, which is later used to analyze the distribution of roots in the complex plane. In Sec. IV, we give a summary of the stability behavior of jets under dc fields; and, after some discussion concerning the choice of nonspurious roots (using the 1-D model), the same study for jets subjected to ac fields. Finally we tackle the practical problem of competition among capillary and resonant modes, including a realistic case. Conclusions are drawn in Sec. V.

II. STATEMENT OF THE PROBLEM

Let us consider an infinitely long liquid column of unperturbed radius R. The outer medium is a gas flowing longitudinally at a relative velocity U_0. The liquid is assumed to be a good conductor, in the sense that its charge relaxation time is much shorter than any other relevant time scale. Consequently, the jet is equipotential for an electroquasistatic situation. A cylindrical electrode of radius bR ($b>1$) is coaxially placed with respect to the jet and an ac electric potential $\Phi_0 \cos(\omega t)$ is established between them. The liquid has arbitrary dynamic viscosity μ and density ρ. Concerning the gas, its density is ρ_g, but viscosity effects are treated as a phenomenological correction to an inviscid model. Both fluids are assumed to be incompressible.

The dynamics of the jet is governed by the continuity and Navier–Stokes equations:

$$\nabla \cdot \mathbf{V} = 0, \quad \rho(\partial_t \mathbf{V} + \mathbf{V} \cdot \nabla \mathbf{V}) = -\nabla P + \mu \nabla^2 \mathbf{V}, \tag{1}$$

where $\mathbf{V}$ and P are the velocity and pressure fields in the liquid. Note that gravity effects are disregarded. For the surrounding gas, which we consider as inviscid for the moment, we have the continuity and Euler equations

$$\nabla \cdot \mathbf{V}_g = 0, \quad \rho_g(\partial_t \mathbf{V}_g + \mathbf{V}_g \cdot \nabla \mathbf{V}_g) = -\nabla P_g, \tag{2}$$

with the subscript "g" standing for the fields in this medium. Note that the presence of an electroquasistatic field does not manifest in these bulk equations but, as we shall see later, in the boundary conditions.[6] This electric field is zero in the conducting liquid; while, in the outer medium, it satisfies

$$\mathbf{E} = -\nabla \Phi, \quad \nabla^2 \Phi = 0. \tag{3}$$

Let us describe the jet shape by the equation $F(\mathbf{r},t)=0$, and the unit normal vector at each surface point as $\mathbf{n}=\nabla F/|\nabla F|$ evaluated at $F=0$. At this locus, the potential Φ is prescribed to

$$\Phi|_{F=0}=\Phi_0\cos(\omega t),$$

assuming that the outer electrode is grounded, i.e., $\Phi|_{r=bR}=0$. Other required boundary conditions are: the kinematic conditions of an evolution of the jet shape consistent with the velocity fields and the equality of their normal components (note that jumps in the tangential components are allowed due to the inviscid treatment of the outer gas),

$$\partial_t F+\mathbf{V}\cdot\nabla F=0,\quad(\mathbf{V}-\mathbf{V}_g)\cdot\mathbf{n}=0;$$

and finally, the stress balance at the free surface,

$$(P-P_g)\mathbf{n}-\mu[\nabla\mathbf{V}+(\nabla\mathbf{V})^t]\cdot\mathbf{n}=\left[\sigma\nabla\cdot\mathbf{n}-\frac{\epsilon_0 E^2}{2}\right]\mathbf{n},$$

where σ is the gas–liquid interfacial tension and the superscript "t" stands for transposition of the corresponding tensor. In the last equation, we can recognize the pressure jump, the viscous stress, the capillary pressure, and the electrostatic pressure terms, respectively. Other general requirements applied at $r=0$ and $r\to\infty$ are that all physical magnitudes are bounded.

As we are interested in a temporal, modal analysis of the jet dynamics, no initial conditions are considered. The unperturbed jet is regarded as an infinite cylindrical column at rest, with a surrounding gas flowing with uniform axial velocity with respect to the former. These features describe a solution of the above equations and boundary conditions, associated with a perfectly cylindrical shape ($F_{\mathrm{cyl}}\equiv r-R=0$). Electric potential and pressure jump are in this case

$$\Phi_{\mathrm{cyl}}(r,t)=-\Phi_0\cos(\omega t)\frac{\ln(r/bR)}{\ln b},$$

$$P_{\mathrm{cyl}}-P_{\mathrm{cyl},g}=\frac{\sigma}{R}-\frac{\epsilon_0\Phi_0^2\cos^2(\omega t)}{2R^2\ln^2 b}.$$

III. STABILITY ANALYSIS

Any small perturbation of the basic solution satisfies a linearized set of equations that we shall present in nondimensional form. Let $\mathbf{v}=(u,v,w)$ and $\mathbf{v}_g=(u_g,v_g,w_g)$ be the perturbation of the basic velocity fields in the liquid and gas, respectively, with explicit decomposition in the local basis of cylindrical coordinates, $\{\mathbf{u}_r,\mathbf{u}_\theta,\mathbf{u}_z\}$. Let also p and p_g be the perturbations of the pressure fields in the liquid and the gas, respectively. The bulk equations in the liquid and in the gas become, respectively,

$$\nabla\cdot\mathbf{v}=0,\quad\partial_t\mathbf{v}=-\nabla p+C\nabla^2\mathbf{v};$$

$$\nabla\cdot\mathbf{v}_g=0,\quad\bar{\rho}\mathcal{D}\mathbf{v}_g=-\nabla p_g,$$

where

$$\mathcal{D}\equiv\partial_t-\sqrt{\mathrm{We}}\,\partial_z.$$

In these equations, we have introduced dimensionless magnitudes using the jet radius R, and the capillary time t_c

$=\sqrt{\rho R^3/\sigma}$ as length and time scales, respectively, and derived scales for the velocity and the pressure fields. Three nondimensional parameters appear in this scheme; namely, the *Ohnesorge number* $C=\mu/\sqrt{\rho\sigma R}$, the density ratio $\bar{\rho}=\rho_g/\rho$, and the *Weber number* $\mathrm{We}=\rho U_0^2 R/\sigma$.

From the fact that both $\mathbf{v}$ and $\mathbf{v}_g$ are solenoidal, the pressure fields are harmonic functions:

$$\nabla^2 p=0,\quad\nabla^2 p_g=0.\tag{4}$$

The gas velocity field is easily obtained once the pressure is known. For the velocity field in the liquid, we find an uncoupled equation by applying the operator ∇^2 to the linearized Navier–Stokes equation, giving

$$\nabla^2[\partial_t-C\nabla^2]\mathbf{v}=0.$$

We propose a solution split into two terms, $\mathbf{v}=\mathbf{v}_v+\mathbf{v}_i$, respectively satisfying the equations

$$[\partial_t-C\nabla^2]\mathbf{v}_v=0,\quad\nabla^2\mathbf{v}_i=0.\tag{5}$$

The fact that the linear operators ∇^2 and ∂_t commute guarantees that the sum of these partial fields satisfies the original equation.

For the electric problem, we have the nondimensional perturbation of the electric potential φ, also satisfying the Laplace equation,

$$\nabla^2\varphi=0.$$

The electric potential has been made nondimensional with the scale RE_0, where $E_0=\Phi_0/[R\ln(b)]$ is the field at the jet surface.

The linearized boundary conditions are now considered. At the z-axis, regularity of the velocity and pressure fields leads to[19]

$$\partial_\theta u|_{r=0}=v|_{r=0},\quad\partial_\theta v|_{r=0}=-u|_{r=0},\quad\partial_\theta w|_{r=0}=0,$$

$$\partial_{\theta z}u|_{r=0}=\partial_z v|_{r=0},\quad\partial_{\theta z}v|_{r=0}=-\partial_z u|_{r=0},$$

$$\partial_{r\theta}w|_{r=0}=\lim_{r\to 0}\frac{\partial_\theta w}{r},\quad\lim_{r\to 0}\frac{\partial_{\theta\theta}w}{r}=-\partial_r w|_{r=0},$$

$$\partial_\theta p|_{r=0}=0,\quad\partial_{r\theta}p|_{r=0}=\lim_{r\to 0}\frac{\partial_\theta p}{r},$$

$$\lim_{r\to 0}\frac{\partial_{\theta\theta}p}{r}=-\partial_r p|_{r=0}.$$

The jet shape is described, also in nondimensional form, by $r=1+f(\theta,z,t)$. At that locus, we impose the kinematic conditions

$$u(r,\theta,z,t)|_{r=1}=\partial_t f,\tag{6}$$

$$u_g(r,\theta,z,t)|_{r=1}=u(r,\theta,z,t)|_{r=1}-\sqrt{\mathrm{We}}\,\partial_z f,\tag{7}$$

and the stress balance at the free surface,

$$C(\partial_z u+\partial_r w)|_{r=1}=0,\tag{8}$$

$$C(\partial_r v-v+\partial_\theta u)|_{r=1}=0,\tag{9}$$

$$p|_{r=1}-p_g|_{r=1}+2C\partial_r u|_{r=1}=-f-\partial_{zz}f-\partial_{\theta\theta}f-\Delta p_E.\tag{10}$$

Here Δp_E is the perturbation of the electrostatic pressure

$$\Delta p_E = -\chi \cos^2(\bar{\omega}t)(f + \partial_r\varphi|_{r=1}),$$

where χ is the electric number, defined as

$$\chi \equiv \frac{\epsilon_0 E_0^2 R}{\sigma},$$

and $\bar{\omega} = \omega t_c$ is the nondimensional field frequency. It is important to note that, since the liquid is perfectly conducting, electric forces only act on the free surface and in its normal direction, so there is no shear stress of electric origin.

A. The dc case

The dc limit ($\bar{\omega} = 0$) of the above problem serves as a first stage in the derivation of the general case ($\bar{\omega} \neq 0$) and, at the same time, constitutes an obligatory reference for a discussion of the results. This case was first published by Saville[7] but here we follow the treatment of García.[8]

The electromechanical dc problem may be solved in two steps. Initially we omit the electrostatic pressure term in Eq. (10) and find the corresponding dispersion relation. Next we evaluate the electrostatic pressure as a function of the free surface shape, f. In fact this term enters the dispersion relation in the same manner as the capillary term, so they are just added. Details will be shown later.

Let us now consider a modal decomposition of all unknowns in the form

$$g(r,\theta,z,t) = \text{Re}[\hat{g}(r)\exp(\Omega t + im\theta + ikz)], \qquad (11)$$

for $g = u_i, v_i, w_i, u_v, v_v, w_v, p, u_g, v_g, w_g, p_g$; and

$$f(\theta,z,t) = \text{Re}[\hat{f}\exp(\Omega t + im\theta + ikz)], \qquad (12)$$

where Ω is a complex eigenvalue whose real and imaginary parts are called *growth factor* and *oscillation frequency*, respectively; m is the *azimuthal number* (integer) and $k = 2\pi R/\lambda$ is the already mentioned nondimensional wave number of the perturbation. Once this modal decomposition is substituted in the set of equations and boundary conditions (4)–(10), we obtain the following problem in the radial variable:

$$\hat{p}'' + \frac{\hat{p}'}{r} - \left(k^2 + \frac{m^2}{r^2}\right)\hat{p} = 0,$$

$$\hat{u}_i'' + \frac{\hat{u}_i'}{r} - \left(k^2 + \frac{m^2+1}{r^2}\right)\hat{u}_i - i\frac{2m}{r^2}\hat{v}_i = 0,$$

$$\hat{v}_i'' + \frac{\hat{v}_i'}{r} - \left(k^2 + \frac{m^2+1}{r^2}\right)\hat{v}_i - i\frac{2m}{r^2}\hat{u}_i = 0,$$

$$\hat{w}_i'' + \frac{\hat{w}_i'}{r} - \left(k^2 + \frac{m^2}{r^2}\right)\hat{w}_i = 0, \qquad (13)$$

$$\hat{u}_v'' + \frac{\hat{u}_v'}{r} - \left(k_v^2 + \frac{m^2+1}{r^2}\right)\hat{u}_v - i\frac{2m}{r^2}\hat{v}_v = 0,$$

$$\hat{v}_v'' + \frac{\hat{v}_v'}{r} - \left(k_v^2 + \frac{m^2+1}{r^2}\right)\hat{v}_v - i\frac{2m}{r^2}\hat{u}_v = 0,$$

$$\hat{w}_v'' + \frac{\hat{w}_v'}{r} - \left(k_v^2 + \frac{m^2}{r^2}\right)\hat{w}_v = 0,$$

where primes mean derivation with respect to r and we define

$$k_v^2 = k^2 + \frac{\Omega}{C}.$$

For the gas pressure field we have

$$\hat{p}_g'' + \frac{\hat{p}_g'}{r} - \left(k^2 + \frac{m^2}{r^2}\right)\hat{p}_g = 0. \qquad (14)$$

The boundary conditions at $r=0$ reduce to

$$\hat{u}(0) = \hat{v}(0) = \hat{w}'(0) = \hat{p}'(0) = 0 \quad \text{(for all } m\text{)},$$

$$\hat{w}(0) = \hat{p}(0) = 0 \quad \text{(for } m=0\text{)}, \qquad (15)$$

while the rest are now written

$$\hat{u}(1) = \Omega\hat{f}, \qquad (16)$$

$$\hat{u}_g(1) = \hat{u}(1) - ik\sqrt{\text{We}}\,\hat{f}, \qquad (17)$$

$$C[ik\hat{u}(1) + \hat{w}'(1)] = 0, \qquad (18)$$

$$C[\hat{v}'(1) - \hat{v}(1) + im\hat{u}(1)] = 0, \qquad (19)$$

$$\hat{p}(1) - \hat{p}_g(1) = (m^2 - 1 + k^2)\hat{f} + 2Cu'(1). \qquad (20)$$

The general solution that satisfies the regularity conditions at $r=0$ and $r\to\infty$ are

$$\hat{p}(r) = -\mathcal{A}\frac{\Omega I_m(kr)}{kI_m'(k)}, \qquad (21)$$

$$\hat{p}_g(r) = -\mathcal{A}_g\frac{I_m(kr)}{kI_m'(k)}, \qquad (22)$$

$$\hat{u}(r) = \hat{u}_i(kr) + \hat{u}_v(k_v r)$$
$$= \mathcal{A}\frac{I_m'(kr)}{I_m'(k)} - \mathcal{B}\frac{I_m'(k_v r)}{I_m'(k_v)} + \mathcal{C}\frac{I_m(k_v r)}{I_m(k_v)}, \qquad (23)$$

$$\hat{v}(r) = \hat{v}_i(kr) + \hat{v}_v(k_v r)$$
$$= \mathcal{A}\frac{imI_m(kr)}{krI_m'(k)} - \mathcal{B}\frac{imI_m(k_v r)}{k_v rI_m'(k_v)} + \mathcal{C}\frac{ik_v I_m'(k_v r)}{mI_m(k_v)}, \qquad (24)$$

$$\hat{w}(r) = \hat{w}_i(kr) + \hat{w}_v(k_v r) = \mathcal{A}\frac{iI_m(kr)}{I_m'(k)} - \mathcal{B}\frac{ik_v I_m(k_v r)}{kI_m'(k_v)}, \qquad (25)$$

where we have used standard notation for the intervening modified Bessel functions; and $\mathcal{A}$, $\mathcal{A}_g$, $\mathcal{B}$, and $\mathcal{C}$ are constants to be determined. Substitution of solutions (21)–(25) into conditions (16)–(20) gives the following algebraic system:

$$\mathcal{A} - \mathcal{B} + \mathcal{C} - \Omega\hat{f} = 0, \qquad (26)$$

$$\mathcal{A} - \mathcal{B} + \mathcal{C} - ik\sqrt{\text{We}}\,\hat{f} = \frac{\mathcal{A}_g}{\bar{\rho}(\Omega - ik\sqrt{\text{We}})}, \qquad (27)$$

Phys. Fluids, Vol. 15, No. 2, February 2003

Stability analysis of conducting jets   399

$$\mathcal{A} - \left(1 + \frac{\Omega}{2Ck^2}\right)\mathcal{B} + \frac{1}{2}\mathcal{C} = 0, \tag{28}$$

$$2m(1 - \xi_m(k))\mathcal{A} - 2m(1 - \xi_m(k_v))\mathcal{B}$$
$$+ \frac{2m^2 + k_v^2 - 2/\xi_m(k_v)}{m}\mathcal{C} = 0, \tag{29}$$

$$\{\xi_m(k)\Omega + 2C[(k^2 + m^2)\xi_m(k) - 1]\}\mathcal{A}$$
$$- 2C[(k_v^2 + m^2)\xi_m(k_v) - 1]\mathcal{B} + 2C\left(\frac{1}{\xi_m(k_v)} - 1\right)\mathcal{C}$$
$$- \frac{K_m(k)}{kK_m'(k)}\mathcal{A}_g + (k^2 + m^2 - 1)\hat{f} = 0, \tag{30}$$

where we have defined the auxiliary function

$$\xi_m(k) = \frac{I_m(k)}{kI_m'(k)}.$$

From Eqs. (26)–(29), we can write all the unknown constants as functions of $\hat{f}$ only:

$$\mathcal{A} = \Omega\left(1 + \frac{2Ck^2}{\Omega}\{1 - \eta_m(k_v)[1 - \xi_m(k_v)]\}\right)G_0^{-1}\hat{f},$$

$$\mathcal{A}_g = \bar{\rho}(\Omega - ik\sqrt{\text{We}})^2\hat{f},$$
$$\tag{31}$$

$$\mathcal{B} = 2Ck^2\{1 - \eta_m(k_v)[1 - \xi_m(k)]\}G_0^{-1}\hat{f},$$

$$\mathcal{C} = 2\Omega\left\{-\eta_m(k_v)[1 - \xi_m(k)] + \frac{2Ck^2}{\Omega}\eta_m(k_v)\right.$$
$$\left.\times[\xi_m(k) - \xi_m(k_v)]\right\}G_0^{-1}\hat{f},$$

with

$$\eta_m(k_v) = \frac{m^2}{2m^2 + k_v^2 - 2/\xi_m(k_v)}$$

and

$$G_0 = 1 - 2\eta_m(k_v)[1 - \xi_m(k)] + \frac{2Ck^2}{\Omega}\eta_m(k_v)$$
$$\times[\xi_m(k) - \xi_m(k_v)].$$

Substitution of all these integration constants in Eq. (30) gives $D_0\hat{f} = 0$, with

$$D_0 \equiv G_0^{-1}\{\xi_m(k)\Omega^2 + 2C\Omega(-1 + \{2k^2 + m^2 - k^2\eta_m(k_v)[1 - \xi_m(k_v)]\}\xi_m(k) + 2\eta_m(k_v)[1 - \xi_m(k)][1 - 1/\xi_m(k_v)])$$
$$+ 4C^2k^2((k^2 + m^2)\{1 - \eta_m(k_v)[1 - \xi_m(k_v)]\}\xi_m(k) - (k_v^2 + m^2)\{1 - \eta_m(k_v)[1 - \xi_m(k)]\}\xi_m(k_v)$$
$$+ \eta_m(k_v)[\xi_m(k_v) - \xi_m(k)][1 - 2/\xi_m(k_v)])\} - 1 + m^2 + k^2 - \bar{\rho}(\Omega - ik\sqrt{\text{We}})^2\frac{K_m(k)}{kK_m'(k)}. \tag{32}$$

The dispersion relation in the absence of an applied electric field is $D_0 = 0$. In the last term of the definition of D_0 we find the expression $(\Omega - ik\sqrt{\text{We}})^2$. The semiempirical introduction of the gas viscosity in the model of Sterling and Sleicher[12] is done by the substitution of this expression by

$$\Omega^2 - \beta k^2\,\text{We} - 2ik\sqrt{\text{We}}\,\Omega,$$

with β being a new parameter to be experimentally adjusted and equal to 0.175 in their case. This modification is only justified for the axisymmetric mode, for which the model has been theoretically conceived and experimentally tested.[12] However, we extend it to nonaxisymmetric modes because the main fact resulting from the viscosity of the outer gas is to eliminate the velocity jump, responsible for the Kelvin–Helmholtz instability for all modes. This qualitative argument does not allow us to maintain the same value for β, so the results obtained for $m \neq 0$ must be considered only tentative.

Taking also into account that the jet velocity must be much higher than the group velocity of perturbations for the temporal analysis to be valid, we have the following simultaneous restrictions in the parameter space:[20]

$$\text{We} > 8 \quad \text{and} \quad \bar{\rho}\,\text{We} < 13.$$

The next step is the addition of the electrostatic (outward) pressure Δp_E to be previous formulation. It is not difficult to show,[6] once the electric potential problem is solved, that this new term has the form $\Delta p_E = -\chi H\hat{f}$, with

$$H = 1 - k\frac{-I_m(kb)K_m'(k) + K_m(kb)I_m'(k)}{I_m(kb)K_m(k) - K_m(kb)I_m(k)}.$$

The new dispersion relation is

$$D_0 + \chi H = 0.$$

B. The ac case

Now we turn to the original problem, for which $\bar{\omega} \neq 0$. The electric number is modified by a factor of $\cos^2(\bar{\omega}t)$ and any of the expressions (11)–(12) are no longer valid. A modal decomposition without any assumption for the temporal dependence is in order:

$$g(r, \theta, z, t) = \text{Re}[\hat{g}(r, t)\exp(im\theta + ikz)],$$

$$f(\theta, z, t) = \text{Re}[\hat{f}(t)\exp(im\theta + ikz)]$$

(again, g stands for any fluid dynamic magnitude other than the free surface of the jet). The general method to deal with problems where periodic coefficients enter the set of govern-

ing equations is the decomposition in a temporal exponential factor and a periodic function of time.[21] In our case, the periodicity of the time-dependent coefficient is $T/2$, with $T=2\pi/\bar{\omega}$, i.e.,

$$\hat{g}(r,t)=\mathrm{Re}[\hat{g}_{T/2}(r,t)e^{\gamma t}], \quad \hat{f}(t)=\mathrm{Re}[\hat{f}_{T/2}(t)e^{\gamma t}], \quad (33)$$

where γ, the so-called *Floquet exponent*, is complex in general. The functions $\hat{g}_{T/2}(r,t)$ and $\hat{f}_{T/2}(t)$ being $(T/2)$-periodic, we perform a Fourier expansion in the form

$$\hat{g}_{T/2}(r,t)=\sum_{n=-\infty}^{\infty} g_n(r)e^{i2n\bar{\omega}t},$$

$$\hat{f}_{T/2}(t)=\sum_{n=-\infty}^{\infty} f_n e^{i2n\bar{\omega}t}.$$

Any of the unknowns has the explicit temporal dependence

$$\hat{g}(r,t)=\sum_{n=-\infty}^{\infty} g_n(r)\exp(\gamma t+i2n\bar{\omega}t),$$

$$\hat{f}(t)=\sum_{n=-\infty}^{\infty} f_n \exp(\gamma t+i2n\bar{\omega}t). \tag{34}$$

Therefore a temporal derivative has the algebraic equivalent factor $\gamma+i2n\bar{\omega}$.

Solutions to system of linear differential equations with periodic coefficients may be subharmonic,[22] this distinguished case corresponds to $\gamma=i\bar{\omega}$.

Note that the substitution of these expansions in Eqs. (4)–(9) gives an independent set of equations for each n ($n=-\infty,...,0,...,\infty$), equivalent to the one in the dc case, given by Eqs. (13)–(19), provided Ω is replaced by $\gamma+2in\bar{\omega}$. Therefore, for each n expressions (21)–(29) and (31), together with the substitutions

$$\Omega\leftarrow\gamma+i2n\bar{\omega} \quad \text{and} \quad \hat{f}\leftarrow\hat{f}_n \tag{35}$$

give us the solution for $\hat{p}_n$, $\hat{p}_{gn}$, $\hat{u}_n$, $\hat{v}_n$, and $\hat{w}_n$ in terms of $\hat{f}_n$.

Now, we are ready to apply the remaining condition, Eq. (30), in which the electric pressure term has now a factor $\cos^2(\bar{\omega}t)$. This factor, which can be expressed as

$$\cos^2(\bar{\omega}t)=\tfrac{1}{2}+\tfrac{1}{4}e^{2i\bar{\omega}t}+\tfrac{1}{4}e^{-2i\bar{\omega}t},$$

couples the equations for different n. If we introduce the Fourier expansion for p, p_g, u_r, and f; and express all the coefficients in terms of the f_n's, we can collect the coefficients of terms having $e^{i2n\bar{\omega}t}$ to obtain the infinite set of difference equations

$$D_n f_n+\tfrac{1}{4}\chi H(2f_n+f_{n+1}+f_{n-1})=0, \tag{36}$$

where D_n comes from the function D_0 once we have made the substitution (35).

The difference equations (36) are solved in terms of continued fractions.[23] To this end, we will consider separately the cases $n=0$, $n>0$, and $n<0$. For $n=0$ we have

$$D_0+\frac{1}{4}\chi H\left(2+\frac{f_1}{f_0}+\frac{f_{-1}}{f_0}\right)=0. \tag{37}$$

For $n>0$ we rearrange Eq. (36) to give

$$\frac{f_n}{f_{n-1}}=\frac{-\chi H/4}{D_n+\dfrac{\chi H}{2}+\dfrac{\chi H}{4}\dfrac{f_{n+1}}{f_n}}.$$

Repeated substitution of the ratios f_{n+1}/f_n for n increasing lead to a continued fraction. Following the book of Abramowitz and Stegun,[22] we define

$$c_f(a_n,b_n)=b_0+\frac{a_0}{b_1+}\frac{a_1}{b_2+}\cdots$$

and we have

$$\frac{\chi H}{4}\frac{f_1}{f_0}=c_f(-\chi^2 H^2/16,D_n+\chi H/2) \quad \text{with} \quad b_0=0.$$

Analogously, for $n<0$,

$$\frac{f_n}{f_{n+1}}=\frac{-\chi H/4}{D_n+\dfrac{\chi H}{2}+\dfrac{\chi H}{4}\dfrac{f_{n-1}}{f_n}}$$

and we find

$$\frac{\chi H}{4}\frac{f_{-1}}{f_0}=c_f(-\chi^2 H^2/16,D_{-n}+\chi H/2).$$

Finally, substitution in Eq. (37) gives

$$D_0+\tfrac{1}{2}\chi H+c_f(-\chi^2 H^2/16,D_n+\chi H/2)$$
$$+c_f(-\chi^2 H^2/16,D_{-n}+\chi H/2)=0, \tag{38}$$

which is an implicit relation determining the values of the Floquet exponents γ as a function of all the relevant parameters.

The roots of Eqs. (38) are not easy to find. Truncation of the two involved continued fractions determines the number and distribution of poles and zeros in the complex plane. A general knowledge of these distributions is needed to find nonspurious roots and to study their convergence with respect to the number of retained terms. A simplified version of the dispersion relation for axisymmetric jets ($m=0$) comes to our assistance in this particular case.

C. Axisymmetric jet: 1-D approach

In this subsection we describe the changes in the dispersion relation, valid for both the dc and ac cases, when using a 1-D model for the dynamics of an axisymmetric jet ($m=0$). Among the 1-D schemes studied by García and Castellanos,[18] the "average model" has proven to be the best choice if accuracy and simplicity are considered together. This model performs a Taylor-series expansion of the velocity field of the liquid in the radial coordinate and retains only terms up to the second power of the variable. Consistent truncation in all the magnitudes and the choice of the free surface and the mean velocity at each section of the jet as the two sole unknowns lead to a very simple formulation of the jet dynamics. Its linearized version allows us to replace Eq. (32) by

$$D_0 = 2\left(1 + \frac{k^2}{8}\right)\frac{\Omega^2}{k^2} + 6C\Omega - 1 + k^2$$
$$- \bar{\rho}(\Omega - ik\sqrt{We})^2 \frac{K_0(k)}{kK_0'(k)} \qquad (39)$$

for the dc problems and the same substitution rule (35) in this expression for the ac problem. No further changes must be considered.

The interesting point in this formula is that we have a polynomial dependence on Ω; consequently all the zeros of the dispersion relation at any level of truncation of the continued fractions are obtained by standard methods. Spurious zeros, an effect of numerical truncation, are easily discerned from persisting ones by comparison for different truncations. Moreover, the persisting approximate zeros from the 1-D model serve as a convergence guide (typical number of terms retained in the continued fractions) to obtain accurate values from the 3-D formulation. All these features are discussed in Sec. IV B.

IV. RESULTS

A. dc fields

The dc problem with negligible influence of an outer medium is analyzed by Saville,[7] and with more detail by García,[8] who discusses the existence of the so-called hydrodynamic modes. For this reason, the analysis of the role of the relevant parameters that we present now is brief, and has the purpose of serving as a reference to understand parametric resonances when we deal with ac fields. Concerning Saville's results, it is perhaps worth to advance that our range of interest for the Ohnesorge number, C, not much greater than 0.1, does not coincide with his, typically greater than 1. In our case, C is limited by experimental conditions for which parametric resonances could be observed, as we shall see later. In any case, this fact does not mean any restriction on the values of C in our computations.

The dispersion relation for the mode m, $d_m(\Omega, k; C, We, \bar{\rho}, \chi, b) \equiv D_0 + \chi H = 0$, implicitly determines the functions $\Omega_m(k)$ in terms of all listed parameters. The dependence with respect to Ω is transcendental, as it appears in the argument of the modified Bessel functions through the variable k_v. For fixed values of the wave number k and the azimuthal number m, a countable, infinite number of roots can be found. Two of them are associated with the surface deformation, and their corresponding eigenmodes will be called "capillary modes." The other eigenmodes have a recirculating velocity field, whose amplitude is typically much greater than the one of a capillary mode with the same amplitude of the shape of the interface. These are the "hydrodynamic modes," whose evolution is mostly dominated by inertia and viscous stresses in the bulk, while capillary and electrical forces usually have a negligible influence. That is why they are always purely damped, i.e., their corresponding eigenvalues are real and negative. Capillary modes are by far the relevant ones in most situations. Their behavior determine the stability limit in k and the typical breakup time, since their eigenvalues usually have the greatest real part.

The existence of hydrodynamic modes has not been reported until recently[8] because of two reasons. First, as their roots in the complex plane lie very close to poles, they are hard to be found. Second, being purely damped, they do not contribute to the rupture of the liquid jet into drops. Thus their role is much less significant and no interesting information is lost if they are ignored. In addition, being their eigenmodes real, they are not able to generate parametric resonance, as it will be clear later.

The physical mechanisms that play a role in the stability of the jet against small perturbations are easily identified in the dispersion relation. Capillary forces are the reference ones; if alone, they make the jet unstable to perturbations with $k < 1$ and stable otherwise (Rayleigh instability). Viscous forces are measured by the Ohnesorge number C, and they do not modify the Rayleigh stability limit but lower the growth rate of any perturbation. The pressure field of the surrounding gas introduces the Kelvin–Helmholtz instability mechanism, identified in the dispersion equation by the term affected by the combination $\bar{\rho}$We. Thus it acts more strongly for higher jet velocities and fluids with more similar densities; this mechanism is well known to be more efficient for greater wave numbers. The nonuniformity of the gas velocity near the free surface is responsible for the loss of efficiency of this mechanism.[12] Finally, electric forces acting on the free surface are measured by the electric number χ; for $m = 0$, we must distinguish two opposite mechanism:[6–8] on the one hand, we have stabilization due to a relative increase of the outward electrostatic pressure in the valleys of perturbations (because the field is greater for thinner columns at a fixed potential); on the other hand, we have destabilization caused by the point effect at the crests. As these two effects are related to the local mean curvature of the jet surface, their dominance depends on the wavelength of the perturbations, so the electrostatic pressure is globally stabilizing for low k and destablizing for high k. The value of k which is the limit between both situations, i.e., neutral electrical effect, is dependent on the parameter b (radius of the outer electrode in units of jet radius), but not greater in any case than $k = 0.595$. For $m = 1$, the cross section is circular and area-preserved and the stabilizing mechanism related to the radial dependence of the field is not present. Higher azimuthal modes, characterized by a corrugation of the peripheral line of the cross section, are hard to be destabilized because the capillary forces act more strongly.

Figure 1 shows a typical stability spectrum for $m = 0$, with the real and imaginary parts of Ω represented separately as functions of the nondimensional wave number k. Stable and unstable regions in the k-axis are easily identified by the sign of Re(Ω). If $\chi > 1$, the outward electrostatic pressure is strong enough with respect to the capillary pressure jump to stabilize a small region near $k = 0$, where we find slightly damped oscillations. In the figure, this region is not noticeable because χ is too close to unity, so it is restricted to $0 \leq k < 0.0077$ and the maximum real and imaginary parts of the eigenvalues are of the order of 2.5×10^{-6} and 5×10^{-4}, respectively. Otherwise ($\chi < 1$), this region has a real positive root leading to aperiodic growth, like the adjacent k-region, up to a value of k increasing with χ and We from
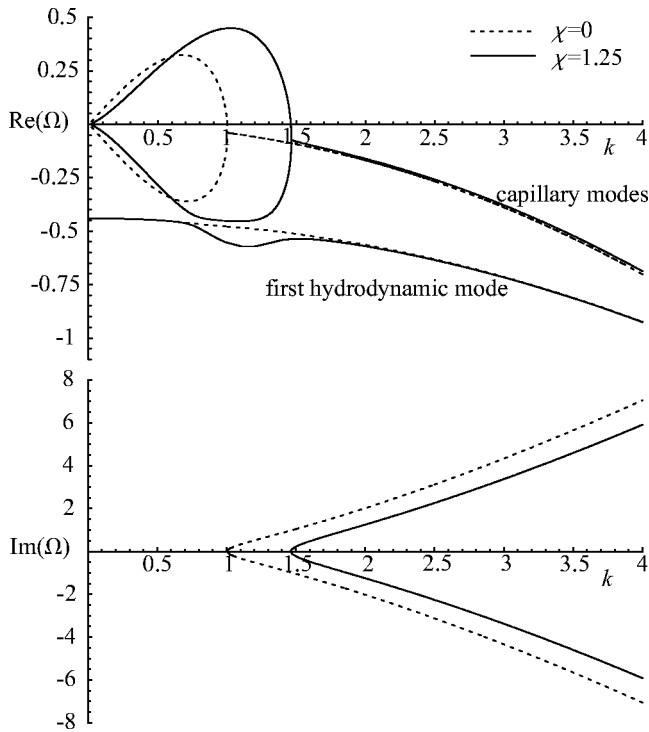
FIG. 1. Nondimensional growth factor Re (Ω) and natural frequency Im (Ω) for the axisymmetric mode ($m=0$) of a jet subjected to a dc field, as a function of the nondimensional wave number k of perturbations. The selected values of the parameters are: $C=0.03$, $b=25$, We$=0$, and $\chi=0$ (dashed line) or $\chi=1.25$ (solid line). Only the first (most significant) hydrodynamic mode from an infinite series is represented.

the Rayleigh stability limit $k=1$ (valid for $\chi=$We$=0$). Beyond this region we find aperiodic damping, except for a k-segment where we have damped oscillations [Im(Ω)$\neq0$]; this segment is not presented for $C>0.573$ if $\chi=$We$=0$, even for lower values when the electric field and/or the influence of the outer medium are considered.

From a practical point of view, the most interesting feature in the dc dispersion relation is the maximum growth rate among all possible perturbations and its corresponding wave
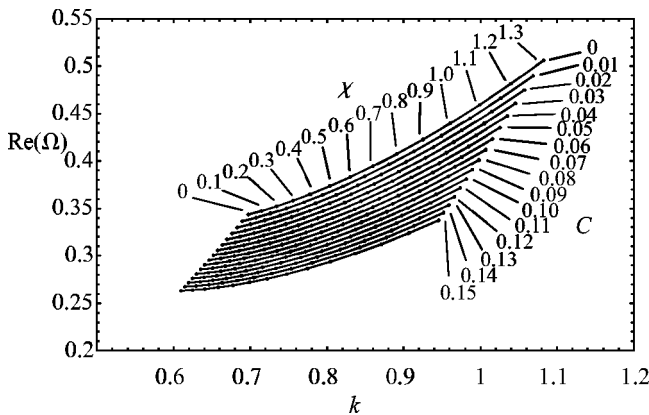

FIG. 2. Maximum growth rate $[\text{Re}(\Omega)]_{\text{max}}$ and corresponding wave number k_{max} for the axisymmetric mode for different values of the parameters C and χ (dc case). The rest of the parameters are fixed to $b=25$ and We$=0$. These magnitudes are the most relevant to determine the unbroken length of a jet and the size of the resulting drops from a natural (noise-driven) breakup process.

number, giving respectively the breakup length of the jet and the size of the resulting drops. A map of these values for different C and χ has been reported by García and Castellanos.[24] In Fig. 2 we reproduce a representative part of that parametric study for the sake of further comparison with ac results. The general behavior shown is an increase of the maximum growth rate and its associated wave number for χ increasing and C decreasing.

The effect of the surrounding gas has not been considered in the previous discussion. The effect over any stability curve is very similar to that of the electrostatic pressure, i.e., an increase in height and length of the unstable lobe for increasing values of $\bar{\rho}$We.

B. ac fields

The parametric instability is clearly originated by a coupling between a natural frequency of the system and the frequency of the imposed electric field.[9] For this reason, hydrodynamic modes are discarded as generators of parametric resonance, since they are purely damped modes. For axisymmetric modes, no relevant information is lost if we substitute the 3-D (transcendental) dispersion relation by the 1-D (polynomial) one. The 1-D approach allows us to analyze the distribution of zeros in a simpler manner.

The Floquet exponent remains multivalued because the complex numbers $\gamma+i2\bar{\omega}n$, with n integer, are equivalent. As a consequence, all roots are ordered in columns, with a vertical separation $2i\bar{\omega}$. Moreover, if γ is a root, so it is its complex conjugate γ^*. These properties imply the restriction of the effective root finding to a strip $0\leq\text{Im}(\gamma)\leq\bar{\omega}$ in the complex plane. If we truncate both continued fractions present in the 1-D ac dispersion relation at the first term, we find an expression whose zeros are identical to those of a polynomial expression of degree six, namely

$$\left(D_0+\frac{\chi H}{2}\right)\left(D_1+\frac{\chi H}{2}\right)\left(D_{-1}+\frac{\chi H}{2}\right)$$
$$-\frac{\chi^2 H^2}{16}(D_1+D_{-1}+\chi H)=0. \tag{40}$$

Similar expressions are found for successive orders of truncation p, giving polynomials of degree $2+4p$. Although the corresponding number of complex roots is also $2+4p$, only some of them are persisting when p is increased, the others being equivalent roots lying outside the strip defined above. A typical scenario in the complex plane is shown in Fig. 3(a) where roots for $p=1$, 2, 3, and 4 are tracked for some values of the parameters leading to resonance. Although some arrangement of roots in columns is apparent, the rule concerning the indetermination in γ is violated due to truncation of the continued fractions. Note that the substitution of $\gamma+2iq\bar{\omega}$ in the infinite set (36), with q an arbitrary integer, leads to an equivalent infinite set of equations (we have merely to rename $n'=n+q$); but if we deal with a truncated set, the equivalence is lost. For $p=1$ the six roots lie in the vertical line defined by the two roots of the dc case; in fact these roots are also roots for $p=1$, as it could be demonstrated from Eq. (40). For $p=2$, only two conjugate roots lie
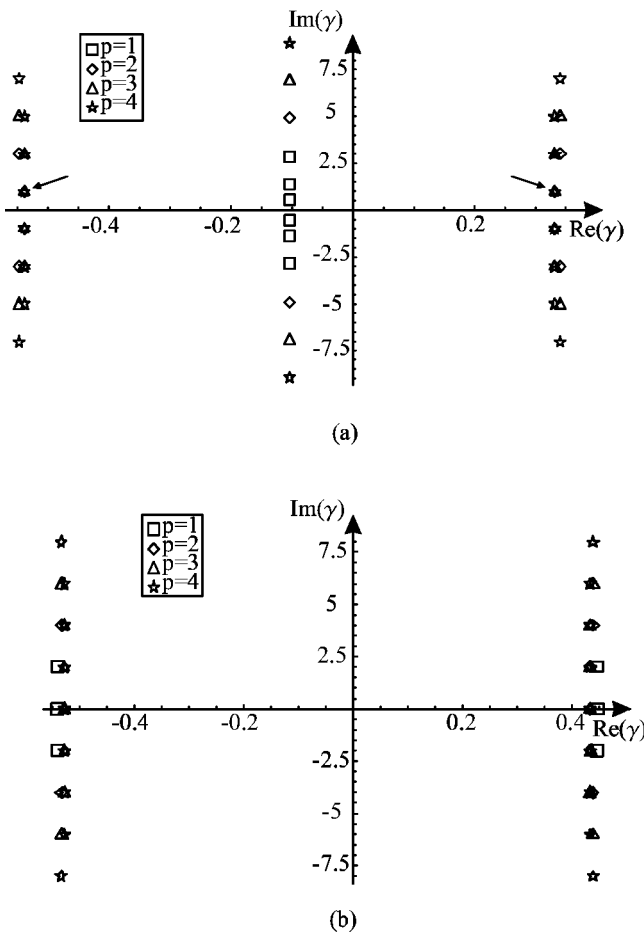
FIG. 3. Distribution in the complex plane of the roots of the ac dispersion relation using the averaged 1-D model. The roots are classified by different marks according to the number p of retained terms in the continued fractions. Parameters are fixed to We=0, b=25, C=0.03, χ=2.5, and $\bar{\omega}$=1. Two different situations are depicted: (a) k=1.8 (resonant) and (b) k=1.1 (nonresonant).

FIG. 4. Stability spectrum from the dispersion relation in the case using the average 1-D model; with C=0.03, b=25, We=0, χ=2.5, and $\bar{\omega}$=1. Real and imaginary parts of the Floquet exponent γ have an analogous meaning as Ω for the dc case (also represented in the figure with dashed lines, for the comparable rms value χ=1.25). Resonances are characterized by lobes in the real part and constants 0 (harmonic) or 1 (subharmonic) in the imaginary part. Resonances are located in the k-axis in segments containing the coincidence of multiples of $\bar{\omega}$ with the dc natural frequency.

in the former vertical line, more separated than those corresponding to p=1, while the remaining eight migrate to two new verticals. When the number of terms retained in the continued fractions increases, the distribution of roots reveals its subsequent tendency: the two roots in the central vertical, having increasing imaginary parts, are spurious; the remaining roots lie near two vertical lines and are persistent, with extremely quick convergence to their final values. Only the closest roots to the real axis, pointed in the figure, are relevant, the other being redundant. In this first example, as Im(γ) results to be equal to $\bar{\omega}$, the instability is subharmonic. In Fig. 3(b) a nonresonant situation is shown. The roots are also organized in two columns, but now only slightly deviated from the positions of the two real dc roots. The ac roots closest to the real axis lie on the axis itself, so the instability is harmonic for them. In view of these facts, we will restrict our findings to the closest roots to the real axis for p>1 (typically we choose p=5), with Im(γ)$\geq$0; and, among them, we will choose the one with greatest real part as the dominant Floquet exponent in the stability analysis.

The root selection that we have just discussed is shown in Fig. 4. Real and imaginary parts of the dominant Floquet exponent are represented as a function of the nondimensional wave number for some values of the parameters, for low k. We find an instability window very similar to the dc one (the dashed line in the same figure); we will refer to it as the "capillary lobe"; the rms part of the electric force is what the jet mainly "feels" for these perturbations, although some departure from the dc curve is apparent at the end of the lobe (the role of the parameter $\bar{\omega}$ will be discussed later). As we increase k, the real part of the Floquet exponent becomes negative and its imaginary part increases up to the value Im(γ)=$\bar{\omega}$, for which the subharmonic resonance takes place. This first resonant lobe reaches its maximum for a wave number close to that one verifying the resonance condition Im(Ω)=$\bar{\omega}$, i.e., natural dc frequency equal to the imposed field frequency. Depending on the electric field strength and the importance of viscous damping, the first resonant lobe encountered may reach positive values, thus leading to instability; or, on the contrary, it may lie entirely in the region below the k axis. The imaginary part remains the same for the first resonant lobe, which is subharmonic, as discussed. Increasing further k, the dc curve is recovered until a new resonant lobe is generated, this time with zero imaginary part (harmonic resonance). We observe the same sequence repeated indefinitely, with resonant lobes growing from the dc basis line; they decrease in height and width very quickly, except when $\bar{\omega}$ is low, as it will be later discussed.

Figure 4 has been obtained from the 1-D model. The asymptotic behavior of the curve for increasing values of k (beyond the capillary lobe and omitting the resonant regions) is not consistent with that presented in Fig. 1 (dc case). The discrepancy must be attributed to the shortcomings of the 1-D model for k not small. The damping factor is, according to Eq. (39), $3Ck^2/(1+k^2/8) \sim 24C$. Conversely, the variational model, valid for arbitrary k, predicts the stronger damping Ck^2 for increasing k. Of course, the exact 3-D model does not present these limitations and agrees with the variational calculations for very low viscosities (Fig. 9 will show an example obtained with the 3-D model, and exhibiting a correct behavior for increasing k).

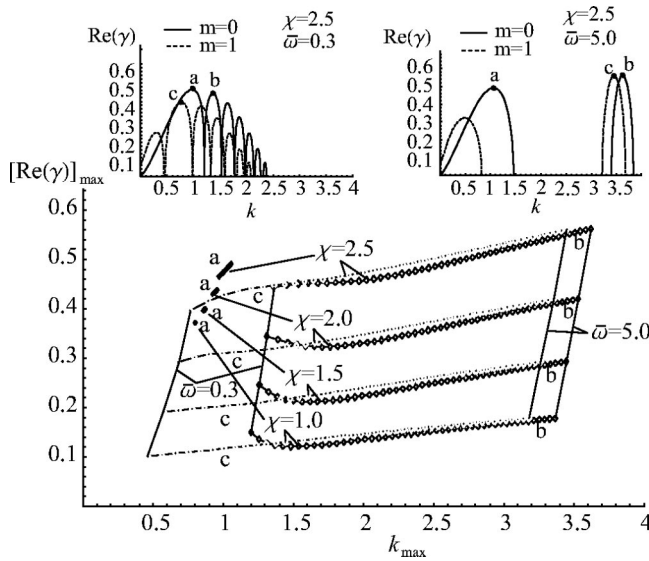If we are interested in experimentally detecting a parametric resonance, the temporal evolution of the free surface should be described and the coefficients $\{f_0, f_{\pm 2}, f_{\pm 2}, \ldots\}$ found. To this end, according to Eq. (36), we select the eigenvector corresponding to the eigenvalue closest to zero of the matrix

$$
\begin{pmatrix}
D_{-n} & & & & & & \\
 & D_{-n+1} & & & & & \\
 & & \ddots & & & & \\
 & & & D_0 & & & \\
 & & & & \ddots & & \\
 & & & & & D_{n-1} & \\
 & & & & & & D_n
\end{pmatrix}
$$

$$
+ \frac{\chi H}{4}
\begin{pmatrix}
2 & 1 & & & & & & \\
1 & 2 & 1 & & & & & \\
 & \ddots & \ddots & \ddots & & & & \\
 & & 1 & 1 & 2 & 1 & & \\
 & & & & \ddots & \ddots & \ddots & \\
 & & & & & 1 & 2 & 1 \\
 & & & & & & 1 & 2
\end{pmatrix},
$$

where the functions D_i $(i=-n,\ldots,n)$ are evaluated at the selected Floquet exponent. In fact, aside from numerical errors, the vector $(f_{-n}, f_{-n+1}, \ldots, f_{n-1}, f_n)$ is the only basis element of the null space of that matrix. The temporal dependence is given by Eq. (34). The number of retained elements need not coincide with the truncation order p, but this choice suffices to achieve a good approximation. What we observe as a general rule is: at the capillary lobe, nonoscillating growth; at the first resonant lobe, oscillations with periodicity $T/2$, growing or decaying depending on the values of the parameters; and, at the second resonant lobe, the same result but with periodicity T. Outside the lobes, the perturbations are decaying, with neither harmonic nor subharmonic periodicity. Figure 5 illustrates these features for the representative cases corresponding to Fig. 4.

1. Comparison with the variational theory

The present results are a generalization of those valid for low viscosities found in Ref. 9. The mathematical approach is quite different in both theories, variational and dynamical,

FIG. 5. Temporal evolution of the free surface amplitude for different representative wave numbers. The selected parameters are the same as in Fig. 4.

so a comparison of results in the range of validity of the former is important in order to know its limits. The variational theory is developed from the basic ansatz that the liquid flow is potential; viscous effects are included via a function that estimates the dissipation in the bulk of the jet.[25] This dominant dissipation is of order C, as it is stated in the evolution equation for the amplitude of perturbations found in Ref. 9, that we transcribe in our present notation for $m=0$ as

$$
\ddot{f} + Cu(k)\dot{f} + d(k,\chi)f = 0, \tag{41}
$$

where $u(k) = 2[2k^2 - 1/\xi_0(k)]$, $d(k,\chi) = -[1-k^2-\chi(t)H]/\xi_0(k)$, and dots mean derivation with respect to time. The dc case $[\chi(t)=\chi_0]$ allows us to estimate errors in this formula from a perturbative expansion in powers of C of the exact dispersion relation $D_0=0$, that we rewrite for $m=0$:

$$
\Omega^2 \xi_0(k) + 4C\Omega\left[k^2 \xi_0(k) - \frac{1}{2} + \frac{Ck^2}{\Omega} \right.
$$
$$
\left. \times (k^2 \xi_0(k) - k_v^2 \xi_0(k_v)) \right]
$$
$$
= 1 - k^2 - \chi H + \bar{\rho}(\Omega - ik\sqrt{\mathrm{We}})^2 \frac{K_0(k)}{kK_0'(k)}. \tag{42}
$$

Aside from the gas effect, which is not included, it can be easily shown that Eq. (41) is the first order expansion in the parameter C of Eq. (42), using the asymptotic expansion of the modified Bessel functions included in $\xi_0(k_v)$ for large values of the argument. The next term in the expansion in powers of C is $-4C^{3/2}\sqrt{\Omega}k^2/\xi_0(k)$, a C-dependence consistent with a viscous dissipation due to the boundary layer adjacent to the free surface.[26] Let us compare the maximum Floquet exponent given by both theories for $\chi=2.5$, $b=25$, $\bar{\omega}=1$, and $C=0.03$. The variational theory gives $(k_{max}, \gamma_{max})=(1.841, 0.290)$ and the dynamical one $(k_{max}, \gamma_{max})=(1.849, 0.323)$; if we estimate the shift in γ_{max} originated by the correction of order $C^{3/2}$, we obtain $\Delta\gamma \approx 4C^{3/2}k^2/[\sqrt{\gamma}\xi_0(k)]=0.047$, which is of the same order as the difference found between both theories. Note that the error of the variational model, some 10%, is not negligible, even for such a low viscosity. As a conclusion, if we seek for

FIG. 6. Dependence of the three competing maximum Floquet exponents on the frequency of the imposed electric field, $\bar{\omega}$. These maxima are marked in the two upper figures as points a (maximum of the capillary axisymmetric lobe), b (maximum of the first resonant axisymmetric lobe), and c (maximum of the first resonant lobe for mode $m=1$). The sweep in frequency goes from $\bar{\omega}=0.3$ up to $\bar{\omega}=5$ in steps of $\Delta\bar{\omega}=0.1$. The rest of the parameters are $We=0$, $C=0$, $b=25$; and $\chi=1$, 1.5, 2, and 2.5.

FIG. 7. Effect of a nonzero viscosity ($C=0.03$) in the study in frequency of Fig. 6 for $\chi=2.5$. The points corresponding to $\bar{\omega}=1.3$ are indicated for a later reference.

a quantitative description of parametric resonance in liquids of non-negligible viscosity, we must use the exact dynamical theory.

2. Modal competition: Role of viscosity and imposed frequency

Previous results obtained from the variational model show that the mode $m=1$ exhibits a first resonance clearly stronger than its capillary lobe and leading to competition with the axisymmetric mode. We first consider these two modes for zero viscosity. The relative maxima are represented in Fig. 6 as a function of the field frequency, in the range $0.3<\bar{\omega}<5$, for different electric numbers χ. The computations are based on initial guesses supplied by the variational method discussed in the latter reference. As pointed before, the capillary lobe has its maximum closely located near the dc limit for the whole range of frequencies. On the other hand, each resonant lobe of both $m=0$ and 1 modes shifts to the right in the k-axis as $\bar{\omega}$ increases, an obvious fact in the light of the above discussion, and the $m=0$ and $m=1$ first lobes tend to join. At the same time, we observe in this figure that their maximum values slightly increase for frequencies not too small. It could be stated that the maximum Floquet exponents of the first resonant lobe for both modes are more similar in size, γ_{max}, and location, k_{max}, as the imposed frequency $\bar{\omega}$ increases. The competition in noise-dominated evolution of jets should presumably consist of a superposition of axisymmetric capillary pinching and deflection of drops with deflection aperture dependent on the growth rate of the mode $m=1$. If a wave number selection mechanism is applied to the jet, with a wave number outside the capillary axisymmetric lobe, axisymmetric nondeflected breakup could be observed provided that the selected wave
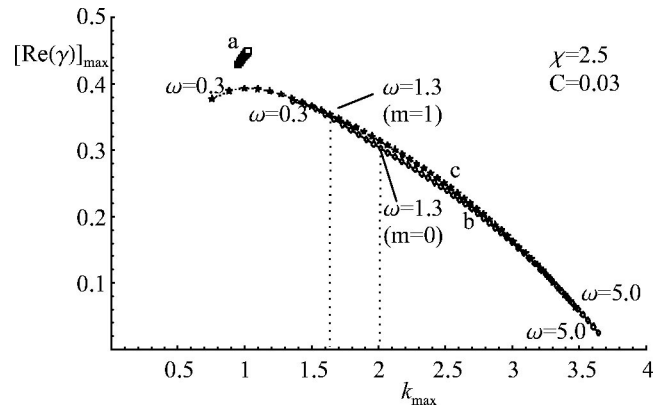
number is very close to the maximum of the $m=0$ resonant lobe and that the $m=1$ resonant lobe is shifted enough (i.e., for a not very high imposed frequency).

One could think, regarding Fig. 6, that high imposed frequencies are desirable to achieve competitive resonances against the capillary rupture. The real fact is that the selection of higher resonant wave numbers makes these unstable modes more affected by viscous damping. To show this, in Fig. 7 we present again the values and location, as a function of $\bar{\omega}$, of the maxima of the first resonant lobes for the modes $m=0$ and 1, as well as the capillary maximum, this time for a nonzero Ohnesorge number ($C=0.03$) and $\chi=2.5$. Even for this low viscosity parameter, the increase observed in Fig. 6 is counterbalanced by viscous damping. Both modes are damped at a similar rate. Saville[7] described for the dc case a stronger viscous damping of capillary perturbations for the mode $m=1$ than for $m=0$, but these findings are not contradictory to ours because resonances take place at higher wave numbers and the range of C considered in each case is not the same (typically $C>1$ in Saville's paper). It is worth noting that the range of viscosities explored in this work is very restricted by the main goal of the determination of physical conditions under which parametric resonances are observable.

Once the basic properties of the induced parametric instability has been elucidated, we turn now to the obtention of numerical results from the exact 3-D dispersion relation. The relevant issue from a practical point of view is again the determination of the wave number of the most dangerous perturbation, along with its growth factor, for the resonant modes. Comparison with the most dangerous capillary mode should determine if the resonance has any chance to be experimentally observed. In Fig. 8, we represent a map of values $(k_{max},[Re(\gamma)]_{max})$ for values of the electric number ($\chi\leq2.5$) and Ohnesorge number C leading to instability for the first resonant lobe. This map has to be essentially compared to that of Fig. 2 (dc case), using there the rms field value ($\chi/2$), because only a small change for the maximum is detected in the capillary lobe. To destabilize liquids with $C\sim0.1$, we need electric fields too hard to be experimentally attained. Only for very low viscosities the resonance has a
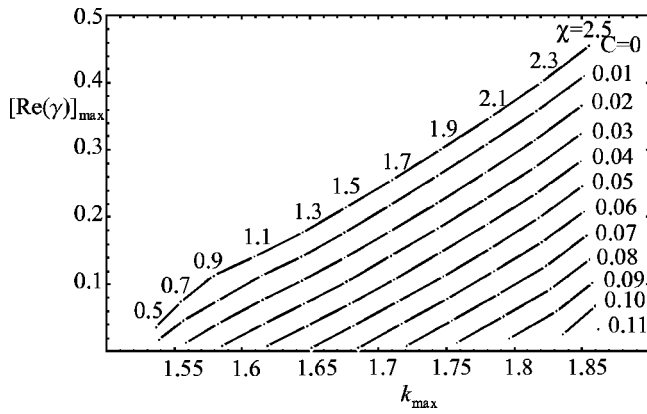
FIG. 8. Map of the maximum growth rate $[\text{Re}(\Omega)]_{\text{max}}$ and corresponding wave number k_{max} for the first resonant lobe of the axisymmetric mode for different values of the parameters C and χ giving positive Floquet exponents. The frequency is set to $\bar{\omega}=1$. The rest of parameters are fixed to $b=25$ and We=0.
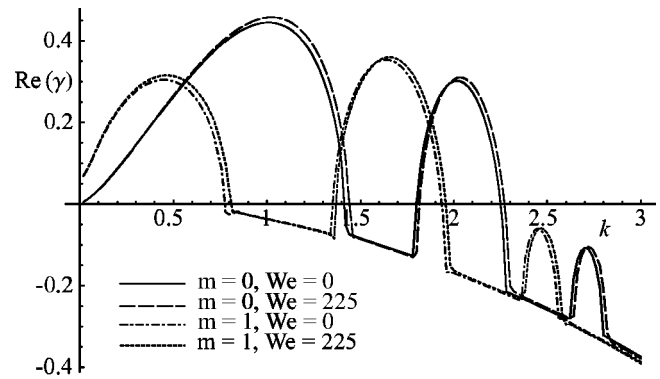

FIG. 9. Growth rates $\text{Re}(\gamma)$ as a function of the nondimensional wave number k for the modes $m=0$ and 1, and We=0 and 225. We used $\bar{\omega}=1.3$, $\bar{\rho}=0.001$; and, for the rest of parameters, the same values as in Fig. 7.

growth factor high enough to be observed, provided the corresponding wave number is previously selected.

For illustration purposes, let us propose a feasible experiment consisting in a conducting jet with a radius $R=100$ μm, density $\rho=1000$ kg/m^3, dynamical viscosity $\mu=16.4$ $\times10^{-4}$ Pa s, and surface tension $\sigma=0.03$ N/m, exiting from a nozzle at a velocity $U_0=8.3$ m/s; these values give $C=0.03$ and We=225. If an outer cylindrical electrode of radius $20R$ is placed coaxially, it can be considered at infinity in order to calculate the highest electric field for which dielectric rupture is prevented. The rupture mechanism in this geometry is a corona discharge occurring at a field evaluated at the jet surface, $E_{0\text{max}}$, and governed by Peek's law[27]

$$E_{0,\text{max}}(\text{kV/cm})=31\left(1+\frac{0.308}{\sqrt{R(\text{cm})}}\right),$$

giving in our case, $E_{0\text{max}}=126.5$ kV/cm and a potential difference between jet and outer electrode $V_0=3.79$ kV. In these conditions, the highest electric number without corona effect is $\chi_{\text{max}}=4.72$. We may thus safely set the appropriate voltage to obtain $\chi=2.5$, a value which has proven, regarding Fig. 7, to generate a first resonance of the order of the maximum of the capillary lobe, at least for not too high field frequencies, for which viscous damping is not severe. More precisely, if we are interested in the generation of an observable resonance leading eventually, after breakup, to drops sensibly smaller than ordinary drops arising from the capillary mechanism, let us choose a nondimensional wave number $k=2$. Figure 7 gives us a value $\bar{\omega}\simeq1.3$ to have the maximum growth rate of the first resonant lobe for that wave number; the corresponding dimensional frequency is 7120 Hz. The question that arises now is about a possible coexistence of resonances for both $m=0$ and $m=1$ modes. The maximum of the first resonance of the mode $m=1$ is not placed at $k=2$, but rather at $k\simeq1.62$, as Fig. 9 shows. Provided the wave number $k=2$ is selected by appropriate stimulation at the nozzle, the only observable resonance is the axisymmetric one ($m=0$). Figure 9 has been constructed with the above calculated values of C, We, χ, and $\bar{\omega}$. If a

sweep in the wave number is experimentally performed, it is expected to observe alternatively lateral and varicose perturbations of the jet, according to the dominance of modes $m=1$ and $m=0$. Also in the same figure, the air effect is measured from comparison between the curves labeled "We=0" and "We=225." Note that the latter are only slightly increased and shifted to the right. We insist in the tentative character of the curve $m=1$, We=225, for which the value $\beta=0.175$ is not justified.

V. CONCLUSIONS

We have presented in this work an exact linear stability analysis of capillary jets of arbitrary viscosity and we have compared it to a previous variational one, valid only for low viscosities. The formulation also included the effect of an outer viscous gas in a semiempirical way. Although the stability spectra predicted by both theories are qualitatively similar, errors in the variational model are significant (about 10%) even for an Ohnesorge number as small as $C=0.03$. For the axisymmetric mode ($m=0$), a one-dimensional model has revealed to be useful to analyze all the roots of the dispersion relation in the complex plane, a difficult task for the 3-D exact model. Once the nature of the roots are analyzed, computations should be performed with the 3-D model due to the applicability of the 1-D model, restricted to the mode $m=0$ and wave numbers not much greater than 1. Modal competition takes place between the capillary axisymmetric ($m=0$) mode and the first resonances of modes $m=0$ and 1, with significant influence of the imposed frequency in the last two ones. Finally, we have shown, by means of a practical case, that experimental evidence of parametric resonances could be pursued.

ACKNOWLEDGMENT

[1]P. Atten and S. Oliveri, "Charging of drops formed by circular jet breakup," J. Electrost. **29**, 73 (1992).
[2]B. Barbet, "Simulation électrohydrodynamique et thermique de jets de liquide conducteur," Thèse doctorale, Université Joseph Fourier, Grenoble, 1997.

[3] D. W. Hrdina and J. M. Crowley, "Drop-on-demand operation of continuous jets using EHD techniques," IEEE Trans. Ind. Appl. **25**, 705 (1989).

[4] C. Bardeau, D. Fressard, P. Atten, and B. Barbet, "Formation of isolated drops in a continuous jet," in IS&T Tenth Int. Congress Adv. Non-Impact Printing Tech., 1994, pp. 429–433.

[5] P. Atten, D. Fressard, B. Barbet, and C. Bardeau, "Electrohydrodynamic induction of isolated drops in a jet," in 9th International Conference on Electrostatics, 1995, Institute of Physics Conf. Ser. 143, York, pp. 47–50.

[6] J. R. Melcher, *Field-coupled Surface Waves* (MIT Press, Cambridge, 1963).

[7] D. A. Saville, "Stability of electrically charged viscous cylinders," Phys. Fluids **14**, 1095 (1971).

[8] F. J. García, "Applicación de modelos unidimensionales a la dinámica de columnas líquidas con y sin campo eléctrico," Tesis doctoral, Universidad de Sevilla, 1998.

[9] H. González, A. Ramos, and A. Castellanos, "Parametric instability of conducting, slightly viscous liquid jets under periodic electric fields," J. Electrost. **47**, 27 (1999).

[10] Lord Rayleigh, "On the capillary phenomena of jets," Proc. R. Soc. London **29**, 71 (1879).

[11] C. Weber, "Zum Zerfall eines Flüssigkeitsstrahles," Z. Angew. Math. Mech. **11**, 136 (1931).

[12] A. M. Sterling and C. A. Sleicher, "The instability of capillary jets," J. Fluid Mech. **68**, 477 (1975).

[13] T. B. Benjamin, "Shearing flow over a wavy boundary," J. Fluid Mech. **6**, 161 (1959).

[14] J. M. Gordillo, M. Pérez-Saborid, and A. M. Gañán-Calvo, "Linear stability of co-flowing liquid–gas jets," J. Fluid Mech. **448**, 23 (2001).

[15] K. Kumar and L. S. Tuckerman, "Parametric instability of the interface between two fluids," J. Fluid Mech. **279**, 49 (1994).

[16] P. Chen and J. Viñals, "Pattern selection in Faraday waves," Phys. Rev. Lett. **79**, 2670 (1997).

[17] J. Miles, "On Faraday resonance of a viscous liquid," J. Fluid Mech. **359**, 321 (1999).

[18] F. J. García and A. Castellanos, "One-dimensional models for slender axisymmetric viscous liquid jets," Phys. Fluids **6**, 2676 (1994).

[19] L Preciosi, K. Chen, and D. D. Joseph, "Lubricated pipelining: stability of core-annular flow," J. Fluid Mech. **201**, 323 (1989).

[20] S. P. Lin and R. D. Reitz, "Drop and spray formation from a liquid jet," Annu. Rev. Fluid Mech. **30**, 85 (1998).

[21] D. D. Joseph, *Stability of Fluid Motions, I* (Springer-Verlag, Berlin, 1976).

[22] M. Abramowitz and I. Stegun, *Handbook of Mathematical Functions* (Dover, New York, 1972).

[23] P. M. Morse and H. Feshbach, *Methods of Theoretical Physics, Vol. 2* (McGraw Hill, New York, 1953).

[24] F. J. García and A. Castellanos, "Effect of interfacial electrical stresses on the stability of viscous liquid jets," in Inst. Phys. Conf. No. 143, 9th Int. Conf. on Electrostat., 1995, pp. 301–304.

[25] L. D. Landau and E. M. Lifshitz, *Fluid Mechanics* (Addison-Wesley, Reading, MA, 1959).

[26] M. Higuera, J. A. Nicolás, and J. M. Vega, "Linear oscillations of weakly dissipative axisymmetric liquid bridges," Phys. Fluids **6**, 438 (1994).

[27] M. Goldman and A. Goldman, in *Gaseous Electronics*, edited by M. L. Hirsh and H. J. Oskam (Academic, Orlando, 1978), Vol. I, Chap. 4, pp. 219–290.